Investigation of the Mg isotopes using the shell-model-like approach in relativistic mean field theory *

Hong-Bo Bai(白洪波)[1;1)] Zhen-Hua Zhang (张振华)[2;2)] Xiao-Wei Li(李晓伟)[1]

[1] Department of Physics, Chifeng University, Chifeng 024001,China

[2] Mathematics and Physics Department, North China Electric Power University, Beijing 102206, China

Abstract: Ground state properties for Mg isotopes, including binding energies, one- and two-neutron separation energies, pairing energies, nuclear matter radii and quadrupole deformation parameters, are obtained from the self-consistent relativistic mean field (RMF) model with the pairing correlations treated by a shell-mode-like approach (SLAP), in which the particle-number is conserved and the blocking effects are treated exactly. The experimental data, including the binding energies and the one- and two-neutron separation energies, which are sensitive to the treatment of pairing correlations and block effects, are well reproduced by the RMF+SLAP calculations.

Keywords: relativistic mean field theory, pairing correlation, shell-model-like approach, Mg isotopes

PACS: 21.60.Jz, 21.10.Dr, 21.10.Re, 21.60.Cs **DOI:** 10.1088/1674-1137/40/11/114101

1 Introduction

In recent years, radioactive ion beams have extended our knowledge of nuclear physics from stable nuclei to exotic nuclei far from the β stability line. Extensive research in this field has been performed, discovering many entirely unexpected features of nuclear structure, such as the halo phenomenon [1] and shell structure involution [2], etc. To understand the new physics in these exotic nuclei, it is very important to find a reliable theory for predicting the properties of the exotic nuclei close to the drip lines.

The relativistic mean field (RMF) theory [3] is one of the most successful microscopic models in the self-consistent description of nuclei. With a few parameters, RMF theory can give a satisfactory description for the ground-state properties all over the nuclide chart for both stable [4, 5] and exotic nuclei [6, 7]. The RMF theory can better reproduce the nuclear saturation properties [8], give a new explanation of neutron halos and proton halos [9, 10], predict giant neutron halos in nuclei close to the neutron drip line [11], give the spin-orbit splitting naturally and explain the origin of the pseudospin and the spin symmetry [12–20], and give a self-consistent description of chiral rotation [21–24] and magnetic and anti-magnetic rotation [25–31].

As an important residual interaction between nuclei, pairing correlations play an essential role in many nuclear properties. Traditionally, the pairing correlations are treated by the Bardeen-Cooper-Schrieffer (BCS) approximation or Hartree-Fock-Bogoliubov (HFB) approach. However, along with their great successes, both BCS and HFB approximations for nuclear pairing raise some concerns [32, 33]. One such concern is the non-conservation of the particle number. Because the number of nucleons in a nucleus is limited, and the number of valence nucleons dominating the nuclear low-lying excited states is even less, the relative particle-number fluctuation is not negligible. Another important concern is the proper treatment of the Pauli blocking effect on pairing, which is responsible for the odd-even differences in nuclear properties. To overcome these drawbacks, a particle-number conserving method [32, 34], namely the shell-model-like approach (SLAP), has been developed. Contrary to the conventional BCS approach, the particle number is conserved and the Pauli blocking effects are taken into account exactly in the SLAP and both odd-A and even-even nuclei can be treated on the same footing. Moreover, exotic nuclei can also be treated by the SLAP when the resonance states are considered. The SLAP has already been implemented in the relativistic mean field (RMF+SLAP) model [35]. SLAP has been employed successfully for describing odd-even differences in moments of inertia (MOIs) [36], the nonadditivity in

Received 15 April 2016

∗ Supported by NSFC (11465001,11275098, 11275248, 11505058,11165001) and Natural Science Foundation of Inner Mongolia of China (2016BS0102)

1) E-mail: baihbcf@sina.com

2) E-mail: zhzhang@pku.edu.cn

MOIs [37, 38], the identical bands [39, 40], the nuclear pairing phase transition [41, 42], the rotational bands and high-K isomers in the rare-earth [43–48], the actinide region and superheavy nuclei [49–52], the cluster structures of light nuclei [53] and the nuclear antimagnetic rotation [54].

Due to a wide span of neutron numbers including 8, 20 and 28 magic numbers, the Mg isotope chain has abundant exotic structures, e.g., island of inversion [55], and halo structure [56, 57], etc. A lot of investigations, such as the shell model [58], the non-relativistic HFB model [59–61] , the relativistic Hartree-Bogoliubov theory and the RMF theory [62–68],etc., have already been performed to investigate the ground state properties of the Mg isotopes. In this work, the RMF+SLAP is adopted to investigate the ground state properties of the Mg isotopes. The paper is organized as follows. A brief introduction to the RMF+SLAP framework is presented in Section 2. Numerical details of the calculation are given in Section 3. The ground state properties for the Mg isotopes are analyzed in Section 4. A brief summary is given in Section 5.

2 Theoretical framework

In the framework of RMF theory, the effective nuclear interaction is usually described by the exchange of the scalar meson σ, the vector meson ω^μ, and the isovector-vector meson $\vec{\boldsymbol{\rho}}^\mu$. The effective Lagrangian density can be written as the following

$$\begin{aligned}\mathcal{L}=&\bar{\psi}\left[\mathrm{i}\gamma^\mu\partial_\mu-M-g_\sigma\sigma-g_\omega\omega^\mu\gamma_\mu-g_\rho\gamma^\mu\vec{\boldsymbol{\tau}}\cdot\vec{\boldsymbol{\rho}}_\mu\right.\\&\left.-e\gamma^\mu\frac{1-\tau_3}{2}A_\mu\right]\psi\\&+\frac{1}{2}\partial^\mu\sigma\partial_\mu\sigma-\frac{1}{2}m_\sigma^2\sigma^2-\frac{1}{3}g_2\sigma^3-\frac{1}{4}g_3\sigma^4\\&-\frac{1}{4}\Omega^{\mu\nu}\Omega_{\mu\nu}+\frac{1}{2}m_\omega^2\omega^\mu\omega_\mu+\frac{1}{4}g_4(\omega^\mu\omega_\mu)^2\\&-\frac{1}{4}\vec{R}^{\mu\nu}\cdot\vec{R}_{\mu\nu}+\frac{1}{2}m_\rho^2\vec{\boldsymbol{\rho}}^\mu\cdot\vec{\boldsymbol{\rho}}_\mu\\&-\frac{1}{4}F^{\mu\nu}F_{\mu\nu}\end{aligned}\tag{1}$$

where the field tensors of the vector mesons and the electromagnetic field take the forms

$$\begin{aligned}\Omega^{\mu\nu}&=\partial^\mu\omega^\nu-\partial^\nu\omega^\mu\ ,\\\vec{R}^{\mu\nu}&=\partial^\mu\vec{\boldsymbol{\rho}}^\nu-\partial^\nu\vec{\boldsymbol{\rho}}^\mu\ ,\\F^{\mu\nu}&=\partial^\mu A^\nu-\partial^\nu A^\mu\ .\end{aligned}\tag{2}$$

According to the Euler-Lagrange equation, the Dirac equation of the nucleon can be written as

$$\{\boldsymbol{\alpha}\cdot\boldsymbol{p}+V(\boldsymbol{r})+\beta[M+S(\boldsymbol{r})]\}\psi_i=\varepsilon_i\psi_i\ ,\tag{3}$$

where ε_i is the single particle energy of the Dirac state i. The scalar $S(\boldsymbol{r})$ and vector $V(\boldsymbol{r})$ potentials are connected in a self-consistent way to various densities through the Klein-Gordon equations for the meson fields $\sigma(\boldsymbol{r})$, $\omega(\boldsymbol{r})$, and $\rho(\boldsymbol{r})$ and the photon fields $A(\boldsymbol{r})$,

$$\begin{cases}\left[-\Delta+m_\sigma^2\right]\sigma(\boldsymbol{r})=-g_\sigma\rho_{\mathrm{s}}(\boldsymbol{r})-g_2\sigma^2(\boldsymbol{r})-g_3\sigma^3(\boldsymbol{r})\ ,\\\left[-\Delta+m_\omega^2\right]\omega(\boldsymbol{r})=g_\omega\rho_v(\boldsymbol{r})-c_3\omega^3(\boldsymbol{r})\ ,\\\left[-\Delta+m_\rho^2\right]\rho(\boldsymbol{r})=g_\rho\rho_3(\boldsymbol{r})\ ,\\-\Delta A(\boldsymbol{r})=e\rho_{\mathrm{p}}(\boldsymbol{r})\ .\end{cases}\tag{4}$$

Following the definition of the Dirac spinors for the axial deformed case in Ref. [35], the scalar and vector densities can be represented as

$$\rho_{s,v}=2\sum_i\left[(|f_i^+|^2+|f_i^-|^2)\mp(|g_i^+|^2+|g_i^-|^2)\right]\ ,\tag{5}$$

where f_i and g_i represent respectively the large and small components of the Dirac state i.

The iterative solution of the Dirac equation for the nucleon and the Klein-Gordon equations for the mesons gives rise to the total energy, quadrupole moments, single-particle energies, etc.

The total energy calculated by the RMF for the system is

$$E_{\mathrm{RMF}}=E_{\mathrm{nucl}}+E_\sigma+E_\omega+E_\rho+E_{\mathrm{c}}+E_{\mathrm{CM}}\ ,\tag{6}$$

with

$$\begin{cases}E_{\mathrm{nucleon}}=\sum\limits_{\mathrm{i}}\varepsilon_{\mathrm{i}}\\E_\sigma=-\frac{1}{2}\int\mathrm{d}^3r\Big\{g_\sigma\rho_{\mathrm{s}}(\boldsymbol{r})\sigma(r)\\\qquad\qquad+\left[\frac{1}{3}g_2\sigma(\boldsymbol{r})^3+\frac{1}{2}g_3\sigma(\boldsymbol{r})^4\right]\Big\}\\E_\omega=-\frac{1}{2}\int\mathrm{d}^3r\{g_\omega\rho_{\mathrm{v}}(\boldsymbol{r})\omega^0(\boldsymbol{r})-\frac{1}{2}g_4\omega^0(\boldsymbol{r})^4\}\\E_\rho=-\frac{1}{2}\int\mathrm{d}^3rg_\rho\rho_3(\boldsymbol{r})\rho^{00}(\boldsymbol{r})\\E_{\mathrm{c}}=-\frac{e^2}{8\pi}\int\mathrm{d}^3r\rho_{\mathrm{c}}(r)A^0(\boldsymbol{r})\\E_{\mathrm{CM}}=-\frac{3}{4}41A^{-1/3}\end{cases}\tag{7}$$

where E_{nucl} is the summation of the energies of nucleon ε_{i}; E_σ, E_ω, E_ρ and E_{c} are the contributions of the meson fields and the Coulomb fields, and E_{CM} is the correction for the center-of-mass motion.

Based on the single-particle levels and wave functions obtained from the Dirac equation (3), the SLAP can be used to treat the nuclear pairing correlations. The Hamiltonian can be written as

$$\begin{aligned} H &= H_{\rm s.p.} + H_{\rm pair} \\ &= \sum_i \varepsilon_i a_i^\dagger a_i - G \sum_{i,j>0}^{i\neq j} a_i^\dagger a_{\bar{i}}^\dagger a_{\bar{j}} a_j \ , \end{aligned} \tag{8}$$

where ε_i is the single-particle energy obtained from the Dirac equation (3), $\bar{i}$ and $\bar{j}$ are the time-reversal states of i and j, and G is the effective pairing strength. This Hamiltonian is diagonalized in a space constructed with a set of multi-particle configurations (MPCs). The MPCs are constructed as the following: the fully paired configuration (seniority $s=0$) for even-even nuclei

$$|\rho_1\bar{\rho}_1\cdots\rho_n\bar{\rho}_n\rangle = a_{\rho_1}^\dagger a_{\bar{\rho}_1}^\dagger \cdots a_{\rho_n}^\dagger a_{\bar{\rho}_n}^\dagger |0\rangle \ , \tag{9}$$

the configurations with two unpaired particles (seniority $s=2$)

$$\begin{aligned} &|i\bar{j}\rho_1\bar{\rho}_1\cdots\rho_{n-1}\bar{\rho}_{n-1}\rangle \\ &= a_i^\dagger a_{\bar{j}}^\dagger a_{\rho_1}^\dagger a_{\bar{\rho}_1}^\dagger \cdots a_{\rho_{n-1}}^\dagger a_{\bar{\rho}_{n-1}}^\dagger |0\rangle \qquad (i\neq j) \ , \end{aligned} \tag{10}$$

and configurations with more unpaired particles (seniority $s=4,6,\ldots$) see e.g., Refs. [32, 35]. The MPC for an odd $N=2n+1$ particle system can be constructed similarly.

In the practical calculations, the MPC space has to be truncated with an energy cutoff $E_{\rm c}$, i.e., the configurations with energies $|E_m - E_0| \leqslant E_{\rm c}$ are used to diagonalize the Hamiltonian (8), where E_m and E_0 are the energies of the mth configuration and the ground-state configuration, respectively.

After the diagonalization of the Hamiltonian (8), one could obtain the nuclear many-body wave function

$$\begin{aligned} |\psi_\beta\rangle = &\sum_{c_1\cdots c_n} v_{\beta,c_1\cdots c_n} |c_1\bar{c}_1\cdots c_n\bar{c}_n\rangle \\ &+ \sum_{i,j}\sum_{c_1\cdots c_{n-1}} v_{\beta(ij),c_1\cdots c_{n-1}} |i\bar{j}c_1\bar{c}_1\cdots c_{n-1}\bar{c}_{n-1}\rangle \\ &+\cdots , \end{aligned} \tag{11}$$

where $\beta=0$ for the ground state, and $\beta=1,2,3,\ldots$ for the excited states. v_β means the coefficient after diagonalization. The pairing energy can be calculated by

$$E_{\rm pair} = \langle\psi_\beta \,|\, H_{\rm pair} \,|\, \psi_\beta\rangle \ , \tag{12}$$

The total energy of the nuclei can be written as

$$E_{\rm total} = E_{\rm RMF} + E_{\rm pair} \ . \tag{13}$$

3 Numerical details

In this work, the ground state properties of twenty-two Mg isotopes with neutron number $N=7-28$ are analyzed systematically by the RMF+SLAP. Axial symmetry is imposed in the present calculations and the Dirac Eq (3) is solved in a space of axially deformed harmonic oscillator basis with 14 major shells and an oscillator frequency given by $\hbar\omega_0 = 41A^{1/3}$. The effective interaction PK1 [69] is adopted. The effective pairing strengths can, in principle, be determined by the odd-even differences in the nuclear binding energies, and are connected with the dimension of the truncated MPC space. The odd-even mass difference is defined, e.g., for the neutron, as:

$$\Delta_n = \frac{1}{2}[B(N-1,Z)+B(N+1,Z)] - B(N,Z) \ , \tag{14}$$

where $B(N,Z)$ is the binding energy of the nucleus with neutron number N and proton number Z. For protons and neutrons, the truncation energy is chosen as $E_c = 40$ MeV. With this truncation, all the most important MPCs in the ground state wavefunction are included. The corresponding proton and neutron effective pairing strengths are chosen as $G_{\rm p} = G_{\rm n} = 10/A$ MeV.

4 Results and discussion

The experimental and the calculated odd-even mass differences for Mg isotopes as function of neutron number N are shown in Fig. 1. The data can be well reproduced by the SLAP+RMF calculations.

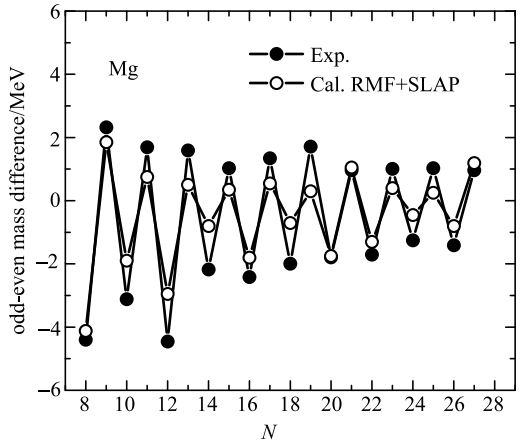

Fig. 1. Experimental and calculated odd-even mass difference for Mg isotopes as a function of neutron number N. The effective pairing interaction strengths for protons and neutrons are $G_{\rm p} = G_{\rm n} = 10/A$ MeV.

The ground state properties of Mg isotopes, including the total binding energy E, the root mean square radii R_m and the quadrupole deformation β_2, from the RMF+SLAP and RMF calculations with effective interaction PK1 are shown in Table 1. The experimental data [56, 70–72] are also shown for comparison. For the ground state, the RMF+SLAP calculations can give a very good description of the data.

Table 1. The experimental and calculated binding energies, radii and quadrupole deformations for the Mg isotope chain. The experimental values of binding energies $E^{\rm exp}$, the root mean square radii $R_m^{\rm exp}$ and quadrupole deformation $\beta_2^{\rm exp}$ are taken from Refs. [56, 70–72].

A	$E^{\rm exp}$/MeV	$E^{\rm RMF}$/MeV	$E^{\rm SLAP}$/MeV	$R_m^{\rm exp}$/fm	$R_m^{\rm RMF}$/fm	$R_m^{\rm SLAP}$/fm	$\beta_2^{\rm exp}$	$\beta_2^{\rm RMF}$	$\beta_2^{\rm SLAP}$
19	−110.927	−113.141	−116.755		2.883	3.010		0.380	0.204
20	−134.468	−134.763	−137.978	2.88	2.830	2.908		0.262	0.010
21	−149.120	−149.884	−150.980		2.852	2.874		0.394	0.379
22	−168.578	−166.895	−167.563	2.89	2.890	2.898	0.580	0.512	0.508
23	−181.726	−180.515	−180.957	2.96	2.901	2.905		0.500	0.498
24	−198.257	−194.628	−195.058	2.79	2.917	2.920	0.605	0.494	0.493
25	−205.588	−203.069	−203.389		2.913	2.915		0.385	0.384
26	−216.681	−212.463	−213.006		2.912	2.919	0.482	0.281	0.286
27	−223.124	−220.459	−220.852	2.90	2.979	2.981		0.320	0.320
28	−231.627	−229.133	−229.691		3.038	3.042	0.491	0.353	0.352
29	−235.299	−234.478	−234.944	3.00	3.088	3.091		0.294	0.294
30	−241.662	−240.390	−241.245	3.06	3.134	3.141	0.431	0.241	0.245
31	−244.040	−244.960	−245.592	3.12	3.171	3.175		0.179	0.180
32	−249.849	−250.368	−251.279	3.12	3.206	3.213	0.473	0.118	0.119
33	−252.071	−252.763	−253.540	3.19	3.274	3.282		0.230	0.235
34	−256.228	−256.766	−257.901	3.23	3.344	3.355		0.340	0.340
35	−256.970	−259.616	−260.475	3.40	3.396	3.405		0.385	0.386
36	−259.740	−262.943	−264.190		3.448	3.463		0.429	0.424
37	−259.999	−263.731	−263.619		3.525	3.534		0.463	0.459
38	−262.314	−264.918	−265.691		3.596	3.596		0.497	0.445
39	−261.807	−266.121	−266.155		3.627	3.640		0.478	0.465
40	−263.240	−267.709	−267.804		3.658	3.680		0.461	0.451

In Fig. 2, the binding energies per nucleon for Mg isotopes from the RMF+SLAP calculations are shown in comparison with the available experimental data [70]. The RMF+SLAP calculations give a very good description of the data except for some nuclei. The binding energy for ^{26}Mg is overestimated a little bit, while the nulei close to the drip line are slightly underestimated.

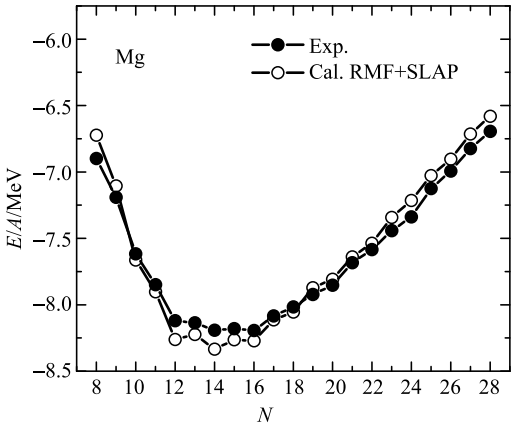

Fig. 2. Experimental and calculated average binding energies for Mg isotopes as a function of neutron number N.

One- and two-neutron separation energies are defined as

$$S_n(Z,N) = B(Z,N) - B(Z,N-1) \tag{15}$$

$$S_{2n}(Z,N) = B(Z,N) - B(Z,N-2)\ , \tag{16}$$

which are very sensitive to test a microscopic theory.

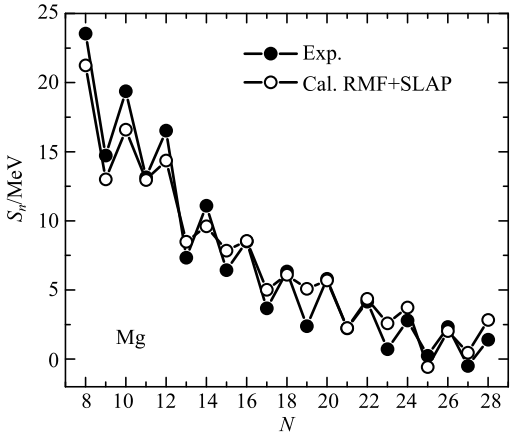

Fig. 3. Experimental and calculated one-neutron separation energies for Mg isotopes as a function of neutron number N.

In Figs. 3 and 4, the one- and two-neutron separation energies from the RMF+SLAP calculations (open circles) with PK1 in comparison with the data (filled circles) are shown. From the figures, it can be seen that the experimental odd-even staggering is well reproduced in

the RMF+SLAP calculations for both the one-neutron separation energy and the two-neutron separation energy. The calculated two-neutron separation energies S_{2n} of Mg isotopes agree reasonably well with the available experimental values except for ^{22}Mg, ^{32}Mg, ^{36}Mg and ^{40}Mg. The large discrepancy in ^{32}Mg is connected to the shape and the shell structure at $N=20$. For the nuclei close to the drip line, the Woods-Saxon basis may be better than the harmonic oscillator basis when solving the Dirac equation (3) [73].

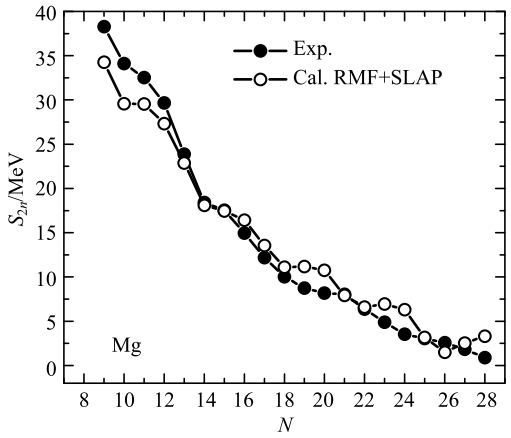

Fig. 4. Experimental and calculated two-neutron separation energies for Mg isotopes as a function of neutron number N.

A comparison of the quadrupole deformation β_2 between the RMF+SLAP calculations and the experimental data is shown in Fig. 5. The experimental data, RMF+SLAP and RMF calculations are denoted by circles, squares and triangles, respectively. The evolution of the quadrupole deformation changing with neutron number is similar in both experimental data and theoretical results. However, the RMF+SLAP calculations are smaller than experimental data. In Ref. [72], the deformation parameter β is determined from the measured $B(\mathrm{E2}:0_1^+\to 2_1^+)$ values,

$$\beta=(4\pi/3ZR_0^2)[B(\mathrm{E2}:0_1^+\to 2_1^+)/e^2]^{1/2} \qquad (17)$$

where the radius R_0 is taken as $1.2A^{1/3}$ fm. However, it has been demonstrated that this empirical relation for the radius is only suitable for medium-mass and heavy nuclei [72]. For light nuclei, the estimation for the radius R_0 is too small, which leads to a large deformation β with Eq. (17). After considering this factor, the consistency between the calculation results and the data will be improved. As for the semi-magic nucleus ^{32}Mg, the data shows a large quadrupole deformation, which turns out to be nearly spherical in both models ($\beta\sim 0.1$). This also results in a large discrepancy from experiment for the two-neutron separation energy S_{2n} of ^{32}Mg, as shown in Fig. 4. Other mean-field models predict spherical shapes for ^{32}Mg, too [65, 66, 74]. For isotopes beyond this nucleus, large deformations are observed, which is related to the quenching of the $N=20$ shell closure. This is the so-called "island of inversion", in which beyond mean field calculations are needed [75].

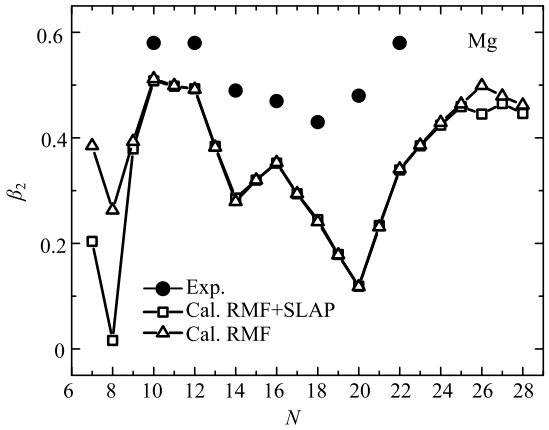

Fig. 5. Experimental and calculated quadrupole deformation parameter β for Mg isotopes as a function of neutron number N. The experimental data, RMF+SLAP and RMF calculations are denoted by filled circles, open squares and open triangles, respectively.

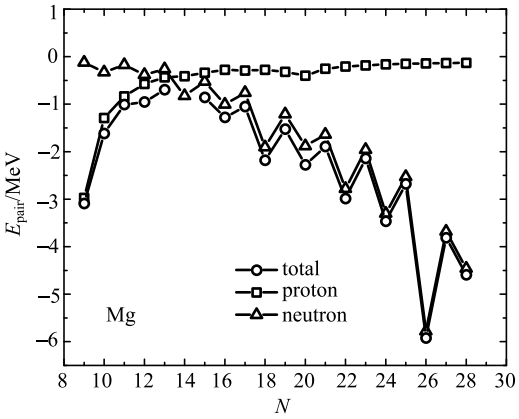

Fig. 6. Total (open circles), proton (open squares) and neutron (open triangles) pairing energies for Mg isotopes as functions of neutron number N, obtained from the RMF+SLAP calculations.

In Fig. 6, the neutron, proton and total pairing energies for Mg isotopes as functions of neutron number N obtained from the RMF+SLAP calculations are shown as open circles, open squares and filled circles, respectively. The neutron pairing energies have an obvious odd-even staggering with increasing neutron number due to the Pauli blocking effect of the unpaired nucleon in the odd-A nucleus, while the proton pairing energy varies smoothly with increasing neutron number N. It can also be seen that neutron pairing energies get larger with

the increase of the neutron number. Hence, in the light Mg isotopes, the proton pairing energy contributes a lot, while in the heavy Mg isotopes the neutron pairing energy is the main part of the total pairing energy. Noted that in the semi-magic nuclei ^{32}Mg and ^{40}Mg, the pairing energies are large, which may indicates disappearances of the traditional magic number at $N = 20$ and 28 in the Mg isotopic chain.

5 Summary

In this work, the ground state properties of Mg isotopes have been investigated using the RMF+SLAP with PK1 effective interaction. These results are also compared with the RMF calculations. The experimental data, including binding energies, one- and two-neutron separation energies, are well reproduced in the RMF+SLAP calculations. The odd-even staggerings in nuclear binding energies and the one-neutron separation energies are well reproduced. The tendency for the quadrupole deformation change with neutron number is consistent between experimental data and theoretical results. The paring energies are also investigated, which indicate that in the light Mg isotopes, the proton pairing energy contributes a lot, while in the heavy Mg isotopes the neutron pairing energy is the main part of the total pairing energy.

The authors are grateful to Prof. Jie Meng for fruitful discussions.

References

1 I. Tanihata H Hamagaki, O Hashimoto et al, Phys. Rev. Lett., **55:** 2676(1985)
2 O. Sorlin, and M. G. Porquet, Prog. Part. Nucl. Phys., **61:** 602(2008)
3 B. B. Serot, and J. D. W., Adv. Nucl. Phys., **16:** 1(1986)
4 P. G. Reinhard, Rep. Prog. Phys., **52:** 439(1989)
5 P. Ring, Prog. Part. Nucl. Phys., **37:** 193(1996)
6 J. Meng, Nucl. Phys. A, **635:** 3(1998)
7 J. Meng, H. Toki, S. G. Zhou et al, Prog. Part. Nucl. Phys., **57:** 470(2006)
8 R. Brockmann, and R. Machleidt, Phys. Rev. C, **42:** 1965(1990)
9 J. Meng,and P. Ring, Phys. Rev. Lett., **77:** 3963(1996)
10 Z. Z. Ren, B. Q. Chen, Z. Y. Ma et al, Phys. Rev. C, **53:** R572(1996)
11 J. Meng, and P. Ring, Phys. Rev. Lett., **80:** 460(1998)
12 A. Arima, M. Harvey, and K. Shimizu, Phys. Lett. B, **30:** 517(1969)
13 K. Hecht,and A. Adler, Nucl. Phys. A, **137:** 129(1969)
14 J. N. Ginocchio, Phys. Rev. Lett., **78:** 436(1997)
15 J. Meng, K. Sugawara-Tanabe, S. Yamaji et al, Phys. Rev. C, **58:** 628R(1998)
16 J. Meng, K. Sugawara-Tanabe, S.Yamaji et al, Phys. Rev. C, **59:** 154(1999)
17 S. G. Zhou, J. Meng, and P. Ring, Phys. Rev. Lett., **91:** 262501(2003)
18 B. N. Lu, E. G. Zhao, and S. G. Zhou, Phys. Rev. Lett., **109:** 072501(2012)
19 B. N. Lu, E. G. Zhao, and S. G. Zhou, Phys. Rev. C, **88:** 024323(2013)
20 H. Liang, J. Meng, and S. G. Zhou, Phys. Rep., **570:** 1(2015)
21 H. Madokoro, J. Meng, M. Matsuzaki et al, Phys. Rev. C, **62:** 061301R(2000)
22 A. D. Ayangeakaa, U. Garg, M. D. Anthony et al, Phys. Rev. Lett., **110:** 172504(2013)
23 I. Kuti, Q. B. Chen, J. Timar et al, Phys. Rev. Lett., **113:** 032501(2014)
24 E. O. Lieder, R. M. Lieder, R. A. Bark et al, Phys. Rev. Lett., **112:** 202502(2014)
25 J. Peng, J. Meng, P. Ring et al, Phys. Rev. C, **78:** 024313(2008)
26 P. W. Zhao, J. Peng, H. Z. Liang et al, Phys. Lett. B, **699:** 181(2011)
27 P. W. Zhao, J. Peng, H. Z. Liang et al, Phys. Rev. Lett., **107:** 122501(2011)
28 P. W. Zhao, J. Peng, H. Z. Liang, et al, Phys. Rev. C, **85:** 054310(2012)
29 J. Meng, J. Peng, S. Q. Zhang,et al, Frontiers Phys., **8:** 55(2013)
30 J. Peng, and P. W. Zhao, Phys. Rev. C, **91:** 044329(2015)
31 P. W. Zhao, S. Q. Zhang, and J. Meng, Phys. Rev. C, **92:** 034319(2015)
32 J. Y. Zeng, and T. S. Cheng, Nucl. Phys. A, **405:** 1(1983)
33 Molique, and J. Dudek, Phys. Rev. C, **56:** 1795(1997)
34 J. Y. Zeng, T. H. Jin, and Z. J. Zhao, Phys. Rev. C, **50:** 1388(1994)
35 J. Meng, J. Y. Guo, L. Liu et al, Frontiers Phys. China, **1:** 38(2006)
36 J. Y. Zeng, Y. A. Lei, T. H. Jin et al, Phys. Rev. C, **50:** 746(1994)
37 S. X. Liu, and J. Y. Zeng, Phys. Rev. C, **66:**067301 (2002)
38 Z. H. Zhang, X. Wu, Y. A. Lei et al, Chin. Phys. C, **32:** 681(2008)
39 S. X. Liu, J. Y. Zeng, and E. G. Zhao, Phys. Rev. C, **66:**024320 (2002)
40 X. T. He, S. Y. Yu, S. X. Liu et al, Chin. Phys. Lett., **21:** 813(2004)
41 X. Wu, Z. H. Zhang, J. Y. Zeng, et al, Phys. Rev. C, **83:** 034323 (2011)
42 L. Liu, Z. H. Zhang, and P. W. Zhao, Phys. Rev. C, **92:** 044304(2015)
43 S. X. Liu, J. Y. Zeng, and L. Yu, Nucl. Phys. A, **735:** 77(2004)
44 Z. H. Zhang, X. Wu, Y. A. Lei et al, Nucl. Phys. A, **816:** 19(2009)
45 Z. H. Zhang, Y. A. Lei, and J. Y. Zeng, Phys. Rev. C, **80:** 034313(2009)
46 Z. H. Zhang, S. T. Qi, B. X. Sun et al, Chin. Phys. C, **34:** 39(2010)
47 Z. H. Zhang, H. Q. Xu, and B. X. Sun, Chin. Phys. C, **34:** 1836(2010)
48 B. H. Li, Z. H. Zhang, and Y. A. Lei, Chin. Phys. C, **37:** 014101(2013)
49 X. T. He, Z. Z. Ren, S. X. Liu, et al, Nucl. Phys. A, **817:** 45 (2009)
50 Z. H. Zhang, J. Y. Zeng, E. G. Zhao et al, Phys. Rev. C, **83:** 011304R(2011)
51 Z. H. Zhang, X. T. He, J. Y. Zeng et al, Phys. Rev. C, **85:** 014324(2012)
52 Z. H. Zhang, J. Meng, E. G. Zhao et al, Phys. Rev. C, **87:** 054308(2013)
53 L. Liu, and P. W. Zhao, Chin. Phys. C, **36:** 818(2012)

54 Z. H. Zhang, P. W. Zhao, J. Meng et al, Phys. Rev. C, **87:** 054314 (2013)
55 C. Thibault, R. Klapisch, C. Rigaud et al, Phys. Rev. C, **12:** 644(1975)
56 R. Kanungo, A. Prochazka, W. Horiuchi et al, Phys. Rev. C, **83:** 021302R(2011)
57 N. Kobayashi, T. Nakamura, Y. Kondo et al, Phys. Rev. Lett., **112:** 242501(2014)
58 E. K. Warburton, J. A. Becker, and B. A. Brown, Phys. Rev. C, **41:** 1147(1990)
59 J. Terasaki, H. Flocard, P. H. Heenen et al, Nucl. Phys. A, **621:** 706(1997)
60 R. Rodríguez-Guzmán, J. L. Egido, and L. M. Robledo, Nucl. Phys. A, **709:** 201(2002)
61 J. C. Pei, Y. N. Zhang, and F. R. Xu, Phys. Rev. C, **87:** 051302(R)(2013)
62 S. Patra, and C. Praharaj, Phys. Lett. B, **273:** 13(1991)
63 Z. Ren, Z. Zhu, Y. Cai et al, Phys. Lett. B, **380:** 241(1996)
64 S. G. Zhou, J. Meng, P. Ring et al, Phys. Rev. C, **82:** 011301R(2010)
65 J. M. Yao, H. Mei, H. Chen et al, Phys. Rev. C, **83:**014308 (2011)
66 L. Li, J. Meng, P. Ring et al, Phys. Rev. C, **85:** 024312(2012)
67 Z. Z. Ren, B. Q. Chen, Z. Y. Ma et al, Z. Phys. A, **353:** 363(1996)
68 X. H. Zhong, Y. H. Tan, and P. Z. Ning, HEP & NP, **27(9):** 794(2003)(in chinese)
69 W. Long, J. Meng, N. V. Giai et al, Phys. Rev. C, **69:** 034319(2004)
70 M. Wang, G. Audi, A. H. Wapstra et al, Chin. Phys. C, **36:** 1603(2012)
71 T. Suzuki, H. Geissel, O. Bochkarev,et al, Nucl. Phys. A, **630:** 661(1998)
72 S. Raman, C. W. NestorJr. and P. Tikkanen, At. Data Nucl. Data Tables, **78:** 1(2001)
73 S. G. Zhou, J. Meng, and P. Ring, Phys. Rev. C, **68:** 034323(2003)
74 T. Nikšić, D. Vretenar, and P. Ring, Phys. Rev. C, **73:** 034308(2006)
75 R. R. Rodríguez-Guzmán, J. L. Egido, and L. M. Robledo, Phys. Rev. C, **62:** 054319(2000)